Colloids and Surfaces B: Biointerfaces 152 (2017) 114–123

Contents lists available at ScienceDirect

Colloids and Surfaces B: Biointerfaces

journal homepage: www.elsevier.com/locate/colsurfb

Topical vaccination with super-stable ready to use nanovesicles

Ayelen Tatiana Caimi [a], Federico Parra [a], Marcelo Alexandre de Farias [b], Rodrigo Villares Portugal [b], Ana Paula Perez [a], Eder Lilia Romero [a], Maria Jose Morilla [a,*]

[a] Nanomedicine Research Program, Departamento de Ciencia y Tecnología, Universidad Nacional de Quilmes, Roque Saenz Peña 352, Bernal, B1876BXD, Argentina
[b] Brazilian Nanotechnology National Laboratory, CNPEM, Caixa Postal 6192, CEP 13.083-970, Campinas, São Paulo, Brazil

ARTICLE INFO

Article history:
Received 11 October 2016
Received in revised form
18 December 2016
Accepted 24 December 2016
Available online 26 December 2016

Keywords:
Archaeolipids
Sterilization
Lyophilization
Cold-free storage

ABSTRACT

Ultradeformable archaeosomes (UDA) are nanovesicles made of total polar archaeolipids (TPA) from the archaea *Halorubrum tebenquichense,* soybean phosphatidylcholine and sodium cholate (3:3:1 w/w). Fresh dispersions of UDA including different type of antigens are acknowledged as efficient topical vaccination agents. UDA dispersions however, if manufactured for pharmaceutical use, have to maintain colloidal stability upon liposomicidal processes such as sterilization and lyophilization ($_{SLR}$UDA), needed to extend shelf life during storage. The remaining capacity of $_{SLR}$UDA to act as adjuvants was therefore tested here for the first time. Another unexplored issue addressed here, is the outcome of replacing classical antigen inclusion into nanovesicles by their physical mixture. Our results showed that UDA behaved as super-stable nanovesicles because of its high endurance during heat sterilization and storage for 5 months at 40 °C. The archaeolipid content of UDA however, was insufficient to protect it against lyophilization, which demanded the addition of 2.5% v/v glycerol plus 0.07% w/v glucose. No significant differences were found between serum anti-ovalbumin (OVA) IgG titers induced by fresh or $_{SLR}$UDA upon topical application of 4 weekly doses at 600 μg lipids/75 μg OVA to Balb/c mice. Finally, $_{SLR}$UDA mixed with OVA elicited the same Th2 biased plus a non-specific cell mediated response than OVA encapsulated within UDA. Concluding, we showed that TPA is key component of super-stable nanovesicles that confers resistance to heat sterilization and to storage under cold-free conditions. The finding of $_{SLR}$UDA as ready-to-use topical adjuvant would lead to simpler manufacture processing and cheaper products. .

1. Introduction

Parenteral vaccination requires of needles to inject controlled amounts of antigen and adjuvant by intramuscular, subcutaneous or intradermal routes [1]. However, the skeletal muscle and subcutaneous tissue, have relatively few professional antigen presenting cells (APC) and the expression of MHC class II and co-stimulatory molecules is absent in myocytes which cannot directly prime T cells [1]. Injectable vaccines require of trained personnel and particularly in developing countries is associated to a risk of transmitting infections, due to the widespread reuse of non-sterile syringes [2]. These facts, added to the complex manufacture process of liquid vaccines, place the development of needle and pain free noninvasive immunization procedures as a top priority for public health agencies [3]. Topical vaccination is attractive since it has the potential to make vaccine delivery more equitable, safer and equally or more efficient than parenteral vaccination [4].

Topical vaccination however, is challenged by the barrier that the *stratum corneum* interposed between antigens-adjuvants and the skin-associated lymphoid tissue (SALT) lying few hundred micrometers depth from skin surface [4,5]. In conventional topical vaccination, the *stratum corneum* is disrupted by harsh physical or chemical means [6,7] and antigens are combined with high doses of powerful immunomodulatory agents such as cholera toxin, *Escherichia coli* heat-labile toxin, or Toll Like Receptors (TLR) ligands, such as imiquimod or bacterial CpG motifs [8]. The intense pro-inflammatory activity of these topical adjuvants may induce adverse skin reactions [9] and autoimmune diseases [10]. On the other hand, the damaged skin barrier causes local irritation potentiating skin infections [11]. These are the main reasons for the delayed clinical developments of topical vaccination.

In this scenario, soft matter having elasto-mechanical properties enabling the penetration of the intact *stratum corneum*, could pave the way towards safer and efficient topical vaccination. Topical ultradeformable liposomes (UDL), made of soybean phosphatidyl-

* Corresponding author.
E-mail address: jmorilla@unq.edu.ar (M.J. Morilla).

http://dx.doi.org/10.1016/j.colsurfb.2016.12.039
0927-7765/

choline (SPC) and edge activators such as sodium cholate (NaChol) have been preclinical employed from the middle 90′s, to induce systemic humoral, cellular, and secretory antigen-specific immune responses [12–17]. Moreover, we previously reported that topical immunization with ovalbumin (OVA) included within ultradeformable archaeosomes (UDA: made of total polar archaeolipids (TPA) extracted from the archaea *Halorubrum tebenquichense* plus SPC and NaChol, 3:3:1 w/w) induces long lasting OVA-specific IgG titers 2 orders higher than those induced by UDL-OVA (OVA included in UDL made of SPC and NaChol, 6:1 w/w, lacking TPA) [18]. A similar trend was found for topical immunization with *Leishmania braziliensis* antigens included in UDA [19]. Topical UDA can penetrate the *stratum corneum* to deliver OVA (MW ∼45 KDa) up to the viable epidermis [20]. Besides, UDA are much more pronouncedly captured by phagocytic cells and immature APC than TPA-lacking nanovesicles [21].

Two major drawbacks, however, are associated to topical vaccination with ultradeformable nanovesicles: their complex manufacture [22] and the poor stability during storage and use, because of the high proportion of surfactants needed to gain ultradeformability [23,24]. The manufacture process of liposomal vaccines consists of antigens suspension in aqueous inner phase [14–16] or its partition within nanovesicles bilayers [17], removal of the free from associated fraction and its quantification. Then, nanovesicles and antigen should be subjected together to vesicle size reduction, sterilization and dehydration. Such processes induce destabilizing effects both on lipid nanovesicles as well as on protein antigens [25]. The antigen inclusion is carried out assuming it is mandatory to elicit a strong antigen-specific immune response, but its avoidance may lead to a much simpler formulations manufacture. Mixing of nanovesicles and antigens, which can be done locally prior to administration, may speed and reduce the cost of industrial manufacture of a final product for topical immunization. On the other hand, nanovesicles intended for pharmaceutical use must retain colloidal, physical and chemical stability for long periods of storage, and if possible, resist to a potential loss of cold chain or, best, to be cold chain-free [25].

TPA are a mixture of *sn*2,3 glycerol ether linked fully saturated polyisoprenoid chains. TPA containing vesicles are more resistant against lipolytic enzymes, hydrolytic or oxidative attacks [26], and against some physical stress like nebulization [27], than TPA-lacking ones. We speculate that TPA may increase the structural stability of ultradeformable bilayers undergoing sterilization, lyophilization and storage. Then, stored as lyophilized, UDA could be rehydrated and mixed with antigen prior to immunization. To test this hypothesis, in this work we submitted UDA to thermal stress of heat sterilization and to freeze and drying stress of lyophilization. Aqueous dispersion of heat sterilized UDA were lyophilized ($_{SL}$UDA) and then stored at 4 and 40 °C. Finally, we screened for immunogenicity of OVA associated to fresh UDA or $_{SLR}$UDA in different ways: OVA included in the aqueous space of UDA, OVA mixed with UDA, OVA and UDA sequentially administered. We showed that TPA is key to confer UDA resistance to heat stress of sterilization and to storage under cold-free conditions. We also confirmed that $_{SLR}$UDA can be used as a ready-to-use topical adjuvant, since no antigen inclusion- only a physical mixture- was sufficient to elicit an antigen-specific systemic immune response.

2. Materials and methods

2.1. Materials

Soybean phosphatidylcholine (SPC, purity > 90%) was a gift from Lipoid, Ludwigshafen, Germany. Sodium cholate (NaChol), Sephadex G-25, Sephacryl S-200, ovalbumin grade V (OVA), Aluminiumnitratenonahydrat ($Al(NO_3)_3 \times 9H_2O$) and Triton X-100were from Sigma-Aldrich, St. Louis, Missouri. Roswell Park Memorial Institute (RPMI) 1640 medium was from Gibco, Life Technologies (New York, USA). 8-hydroxypyrene-1,3,6-trisulfonic acid (HPTS) was from Molecular Probes (Eugene, Oregon). DPX (*p*-Xylene-Bis-Pyridinium Bromide) was from Thermo Fisher Scientific, Waltham, USA. Ficoll was from GE Healthcare, Munich, Germany. Hypaque was from Winthrop Products, Buenos Aires, Argentina. Glycerol was from ICN Biomedicals Inc. Aurora, Ohio. Glucose, mannose and trehalose were from Anedra, Argentina. Fetal calf serum (FCS), antibiotic/antimycotic solution (penicillin 10,000 IU/mL, streptomycin sulphate 10 mg/ml, amphotericin B 25 μg/ml), glutamine, and trypsin/ethylenediaminetetraacetic acid were from PAA Laboratories GmbH (Pasching, Austria).

2.2. Archaebacteria growth, extraction, and characterization of total polar archaeolipids

Halorubrum tebenquichense archaea, isolated from soil samples of Salina Chica, Península de Valdés, Chubut, Argentina were grown in basal medium supplemented with yeast extract and glucose at 37 °C. Biomass was grown in 15 L media in a 25 L home-made stainless steel bioreactor and harvested after 96 h growth. Total polar archaeolipids (TPA) were extracted from biomass using the Bligh and Dyer method modified for extreme halophiles [28]. Between 400 mg and 700 mg TPAs were isolated from each culture batch. The reproducibility of each TPA-extract composition was routinely screened by phosphate content [29], and electrospray-ionization mass spectrometry, as described by Higa et al. [18].

2.2.1. Preparation and characterization of nanovesicles

2.2.1.1. Preparation. Archaeosomes (ARC) made of TPA, ultradeformable liposomes (UDL) made of SPC:NaChol 6:1 (w/w), ultradeformable archaeosomes (UDA) made of SPC:TPA:NaChol 3:3:1 (w/w) and liposomes (L) made of SPC were prepared by the film hydration method. Briefly, mixtures of lipids (60 mg of TPA for ARC; 120 mg of SPC and 20 mg NaChol for UDL; 60 mg of TPA, 60 mg of SPC and 20 mg of NaChol for UDA and 60 mg of SPC for L) were dissolved in 3 ml of chloroform:methanol 1:1 v/v. Then solvents were rotary evaporated at 40 °C until elimination. The lipid films were flushed with N_2 and hydrated with 3 ml of aqueous phase (10 mM Tris-HCl buffer pH 7.4 with 0.9% w/w NaCl –Tris-HCl buffer) up to a final concentration of 40 mg/ml total lipids for UDA and UDL, and 20 mg/ml for ARC and L. The resultant suspensions were sonicated (1 h with a bath-type sonicator 80 W, 80 KHz) and extruded 10 times through a sandwich of 0.2 μm and 0.1 μm pore size polycarbonate filters using a Thermobarrel extruder (Northern Lipids, Vancouver, Canada).

To prepare ovalbumin containing nanovesicles (UDA-OVA), lipid films were hydrated with 3 ml of 6 mg/ml of OVA in Tris-HCl buffer. Free OVA was removed from OVA-UDA by gel filtration on Sephacryl S-200 using the minicolumn centrifugation technique [30]. Briefly, aliquots of 300 μl of UDA-OVA were seed on a 3-ml syringe filled with Sephacryl-S200 and centrifugated during 3 min at 700 x g. Fractions of 240–300 μl were collected upon elution with 300 μl of Tris HCl buffer pH 7.4. The elution profile was determined by quantifying proteins and phospholipids in each fraction.

To prepare HPTS/DPX containing UDA and UDL (HPTS/DPX-nanovesicles), lipid films were hydrated with solution of 35 mM HPTS and 50 mM DPX in Tris-HCl buffer pH 8.7. Free HPTS and DPX were removed from HPTS/DPX-nanovesicles by gel filtration on Sephadex G-25 using the minicolumn centrifugation technique, as described before.

2.2.1.2. Size and Z potential. Size and Zeta potential were determined by dynamic light scattering (DLS) and phase analysis light

scattering (PALS) respectively, using a nanoZsizer (Malvern Instruments, Malvern, UnitedKingdom). Samples were diluted 1:20 in Tris-HCl buffer pH 7.4 (50 μl of samples with 950 μl of Tris-HCl buffer) for size and Z potential determinations.

2.2.1.3. Quantification of phospholipids, OVA and HPTS. Phospholipids were quantified by a colorimetric phosphate microassay [29].

OVA was quantified, by the BCA method employing a commercial kit (Micro BCA™ Protein Assay Kit, Thermo Scientific), on delipidated samples [31,32]. Briefly, 100 μl UDA-OVA were poured in an eppendorf tube followed by 400 μl methanol, 400 μl chloroform and 220 μl water. After vigorous vortexing, tubes were centrifuged 3 min at 9000 × *g*, the upper phase was removed and 600 μl methanol was added. Upon a second centrifugation step, the supernatant was removed, and the resulting protein pellet was dried under nitrogen flux. The precipitate was solubilized in 5% SDS and quantified.

HPTS was quantified by spectrofluorometry (λ_{Ex} 413 nm and λ_{Em}515 nm) before and after complete disruption of nanovesicles in 10% v/v Triton X-100. The fluorescence intensity (FI) of the sample, calculated as FI with Triton X-100 − FI without disruption, was compared to a standard curve prepared with HPTS-DPX in solution. The standard curve was linear in the range 0.18–12 μM HPTS with correlation coefficient of 0.996.

2.3. Freeze-thawed and lyophilized-rehydrated nanovesicles

Fresh nanovesicles were frozen in the absence and presence of glycerol alone or in combination with glucose, mannose and trehalose. Amounts of 6.3 mg of sterile glycerol were weighed and the nanovesicles or nanovesicles-carbohydrate mixture (0.07% w/v for glucose and sucrose and 0.14%w/v for trehalose, at a lipid to carbohydrate ratio of 10:1 mol:mol, corresponding to 4 mM carbohydrate) was added to the tube up to a final glycerol concentration of 2.5% v/v (3.15% w/v). In all cases, aliquots of 200 μl were frozen at −80 °C for 24 h. Part of the samples were thawed at room temperature, and the other were lyophilized (−80 °C and 0.05 mbar) for 48 h using a Freeze Dryer Unit Gamma A instrument (Martin Christ, Germany). Before use, lyophilized samples were rehydrated in bidistilled water to the initial lipid concentrations. The rehydration process was completed within 30 s by repeated vortexing.

UDA and UDL loaded with HPTS-DPX were also submitted to freeze and lyophilization in the presence of glycerol and glucose, as stated above, and the release of HPTS after thawing and rehydration was measured as stated before.

2.4. Thermal analysis

Temperature of phase transitions (Tm) and the associated change of enthalpy (ΔHcal) of fresh and lyophilized with and without glycerol-glucose nanovesicles, solid and rehydrated were determined by differential scanning calorimetry (DSC), from −80 to 50 °C at 5 °C/min rate, in a Mettler Toledo DSC 822.

2.5. Morphology

The morphology of fresh and lyophilized rehydrated in glycerol-glucose nanovesicles was conducted by cryo-transmission electron microscopy (cryo-TEM) and TEM.

Cryo-TEM: Samples were prepared in a controlled environment vitrification system Vitrobot Mark IV (FEI, The Netherlands) with controlled temperature (22° C) and humidity (100%). Images were acquired on a Jeol JEM-1400Plus (JEOL, Japan) instrument, operating at 120 kV using a CCD camera GatanMultiScan 794. Image collection and measurements were made with Digital Micrograph (Gatan-USA). Images were not processed after acquisition. Sample preparation and data acquisition were performed at the Electron Microscopy Laboratory (LME)/Brazilian Nanotechnology National Laboratory (LNNano).

TEM: Samples were deposited over a carbon grid. A drop of phosphotungstic acid (0.5% w/v) was deposited over samples for 1 min and then, grids were air-dried and analyzed using a Jeol 1200-EX II (JEOL, Japan) instrument.

2.6. Heating and sterilization of nanovesicles

Suspension of nanovesicles were placed in Eppendorf tubes, loosely covered by a screw cap, allowing the pressurized steam contact with samples. Nanovesicles were autoclaved in a VZ 100 (Villar y Zaurdo S.R.L. Buenos Aires, Argentina) instrument for 15 min at 121 °C. After autoclaving, samples were incubated at room temperature for 1 h before size and HTPS content were measured. Nanovesicles were also submitted to heat by incubation at 80 °C for 6 h in a water bath.

UDA and UDL loaded with HPTS-DPX were also submitted to sterilization or heating at 80 °C, and the release of HPTS was measured as stated before.

2.7. Deformability

Deformability (*D*) of nanovesicles was calculated according to Van den Bergh [33], as $D = J(rv/rp)^2$, where J is the rate of penetration through a permeability barrier, rv is the size of nanovesicles after extrusion, and rp is the pore size of the barrier. To measure J, nanovesicles were extruded through two stacked 50 nm (rp) membranes at 0.8 MPa using a Thermobarrel extruder. Extruded volume was collected along 15 min, each fraction was quantified for phospholipids, and J calculated as the area under the curve of the plot of recovered phospholipids as a function of time. The average vesicle diameter after extrusion (rv) was measured by DLS.

2.8. Stability upon storage

The colloidal stability of aqueous suspension and solid sterilized lyophilized nanovesicles was determined after 5-month storage at 4 °C and 40 °C. Nanovesicles size, PDI and Z potential before and after storage were determined as stated before.

2.9. Immunization

2.9.1. Animals and immunizationschemes

Male 4–6-week-old Balb/c mice were obtained from Facultad de CienciasVeterinarias (UNLP). Mice were housed 5 per cage and kept in a ventilated room under controlled conditions at constant room temperature 22 °C, with 12/12 h light-dark cycle and free access to food and water. The study was conducted following the National Institutes of Health guide for the care and use of Laboratory animals. Five mice per group were topically immunized as follows: i: UDA with OVA incorporated in the aqueous content; ii: UDA mixed with OVA; iii: sequential administration of UDA followed 1 h later of OVA; iv: sterilized, lyophilized, rehydrated UDA mixed with OVA; v: UDL mixed with OVA; and vi: sterilized, lyophilized, rehydrated UDL mixed with OVA. Topical nanovesicles were dropped on manually trimmed hair, intact back skin surface of each mouse over an area of 2 cm^2. Mice were kept in individual cages for 30 min until drops had dried. Topical administrations were done once a week for four weeks (prime), then animals received one boost on day 42. Each dose consists of 75 μg OVA and 600 μg lipids.

Subcutaneous immunization with OVA mixed with ARC and intramuscular immunization with OVA mixed with $Al(OH)_3$ (5 mg),

used as parenteral controls, were done on day 0 and 21, then animals received one boost on day 42.

2.9.2. Total IgG and isotypes determination

Blood was collected from the tail veins at weekly intervals up to 10 weeks, and IgG antibody and isotypes were analyzed by enzyme-linked immunosorbent assay (ELISA). Briefly, microtiter plates were coated overnight at 4 °C with 45 μg/ml antigen in 0.1 M carbonate-bicarbonate buffer (pH 9.6) and then, after washing with PBS containing 0.05% Tween 20 (0.05% PBST), were blocked for 1 h at 37 °C with PBST. After another washing, 100 μl of three-fold dilutions of individual sera in 0.05% PBST was added.After 2 h at 37 °C and further washing, the plates were incubated for 1 h at 37 °C with horseradish peroxidase-conjugated goat anti-mouse IgG (Millipore- Chemicon International, Temecula, California) diluted 1:5000in 0.025% PBST. To determine the antibody isotyping, horseradish peroxidase-conjugated rat anti-mouse IgG1 or IgG2a revealing antisera (PharMingen, San Diego, California), diluted 1:5000, were used. The plates were further washed and incubated with ABTS [2,2′-azino-bis (3-ethylbenzthiazoline-6-sulphonic acid), Sigma] for 10 min at room temperature (20°–25 °C) in the dark. The absorbance was measured at 405 nm using a microplate reader. Antibody titers were represented as end-point dilutions exhibiting an optical density of 0.3 units above background.

2.9.3. Cellular response

The day 35 (post-prime) and day 49 (post-boost), mice were sacrificed and the splenocytes were obtain employing a Ficoll-Hypaque solution according to Boyurn [34]. Briefly, the spleens were disaggregated on a metal mesh employing non supplemented RPMI media (RPMI). The splenocytes were isolated by centrifuging 30 min at 1600 rpm (4 °C) in a Ficoll gradient (1.098 g/ml density) in a Gelec G144d centrifuge. The resultant pellet was washed twice with RPMI and finally suspended in supplemented RPMI (10% SFB; 100 μ/ml penicillin; 100 mg/ml streptomycin; 50 μM 2-mercaptoethanol). The cells were counted in a Neubauer chamber employing Türkdye and seeded in 96 wells plaque with U shape bottom at a density of 3×10^5 cells per well in a final volume of 200 μl. The cells were re-stimulated with 50 μg/ml OVA and concanavalin A (5 μg/ml) as positive control. Non-stimulated cells were used as negative control. After 48 h the supernatants were collected and stored at − 80 °C.

The release of IFN-γ in cells supernatant was measured by ELISA (BD OptEIA™, BD Biosciences, San Jose, CA, USA) following the manufacturer instructions. Absorbance measurements were carried out at 450 nm in a microplate reader.

2.10 Statistical analysis

Statistical analyses were performed by independent two-sample Student *t*-test, two-way analysis of variance (ANOVA) followed by Sidak'smultiple comparisons or one-way ANOVA followed by Dunnet's test using Prisma 4.0 Software (Graph Pad, San Diego, California). *p*-value less than 0.05 was considered statistically significant. *p < 0.05; **p < 0.01; ***p < 0.001; ****p < 0.0001; n.s. represents not significant (p > 0.05).

3. Results

3.1. Freeze-thawed and lyophilized-rehydrated nanovesicles

The colloidal stability of nanovesicles may be lost after freeze and thawed (FT) or lyophilized and rehydrated (LR) [35]. Hence, colloidal stability of unprotected (without cryo/lyoprotectants) FT and LR nanovesicles was determined in terms of size, polydispersity (PDI) and Z potential. We observed the size of FT UDA was 2 fold increased and PDI remained below 0.5, but the size of FT UDL was 6 fold increased and PDI increased to ∼1 (Fig. 1A). The size of LR UDA and LR UDL on the other hand, was several fold increased, together with the PDI (Fig. 1B). These results suggested that UDA had slight higher stability than UDL only after FT. The LR process, on the other hand, destabilized equally the two types of nanovesicles.

Table 1
Thermotropic parameters of fresh, lyophilized and lyophilized and rehydrated nanovesicles.

Formulation	Process	Tm (°C)	ΔH (KJ/mol phospholipids)
UDA	Fresh	−25.4	47.8
	L	−3.91	2.4
	LR	−23	18.8
	L in glycerol-glucose	−19	18
	LR in glycerol-glucose	−18.6	21.6
UDL	Fresh	−25.8	22.8
	L	−37	3.1
	LR	np	np
	L in glycerol-glucose	−11.5	0.8
	LR in glycerol-glucose	np	np

L: lyophilized; LR: lyophilized and rehydrated; np: no peak.

The colloidal stability of nanovesicles after adding glycerol as cryoprotectant, was next determined. We observed that FT UDA and FT UDL retained original size and PDI remained below 0.25. Identical results were obtained by combining glycerol with small amounts of sugars (glucose, mannose or trehalose). Glycerol alone however, was insufficient to stabilize nanovesicles against LR, since size and PDI of LR UDA and LR UDL was 5 fold increased. This time, the combination of glycerol with small amounts of sugars was effective to keep the size of nanovesicles below 250 nm; PDI however, remained low when protected with glycerol-glucose only. In particular, the cryoprotection factor (cf), calculated as the LR/fresh nanovesicles size ratio, was close to 1 for glycerol-glucose (2.5% v/v glycerol and 0.07% w/v glucose) for both LR UDA and LR UDL. Overall, glycerol was sufficient to fully stabilize FT nanovesicles, but glycerol plus small amounts of sugars was required to stabilize LR nanovesicles. No significant changes in Z potential were detected but the HPTS content of LR UDA and LR UDL was completely lost in the presence of glycerol-glucose.

The DSC scanning of fresh nanovesicles UDA and UDL showed phase transition temperatures (Tm) of −25.4 °C and −25.8 °C and melting enthalpies (ΔH) of 47.8 KJ/mol and 22.8 KJ/mol, respectively (Table 1). Since archaeosomes (nanovesicles fully made of TPA) display unusually high melting enthalpy values, in the order of 760 KJ/mol (unpublished data), the high ΔH of UDA could be ascribed to its 43% by weight content of TPA. Synthetic diphytanoyl phospholipid, such as diphytanoylphosphatidylcholine (DPhPC), form highly packed and ordered bilayers because of the interdigitation of the methyl-functionalized chains [36]. Strong Van der Waals interactions between the homogeneous mixture that phytanoyl chains of TPA and acyl chains of SPC form, may explain the high ΔH of UDA.

We observed that unprotected (without glycerol-glucose) UDA and UDL behaved thermodynamically different to lyophilization. As expected, lyophilized unprotected UDA showed Tm of −4 °C, an increase of 21 °C compared to Tm of fresh UDA. Upon rehydration, the Tm of unprotected UDA returned to its original value (−23 °C) (Table 1). Lyophilized unprotected UDL however, showed a Tm of −37 °C, a decrease of 12 °C compared to Tm of fresh UDL. Upon rehydration the phase transition of UDL disappeared.

We also observed that protected (with glycerol-glucose) UDA and UDL also behaved thermodynamically different to lyophilization. Lyophilized protected UDA showed a Tm similar to that of fresh UDA (−19 °C vs −25 °C), while ΔH was reduced nearly to the half (18 KJ/mol). Upon rehydration, both Tm and ΔH remained unchanged. On the other hand, lyophilized protected UDL increased

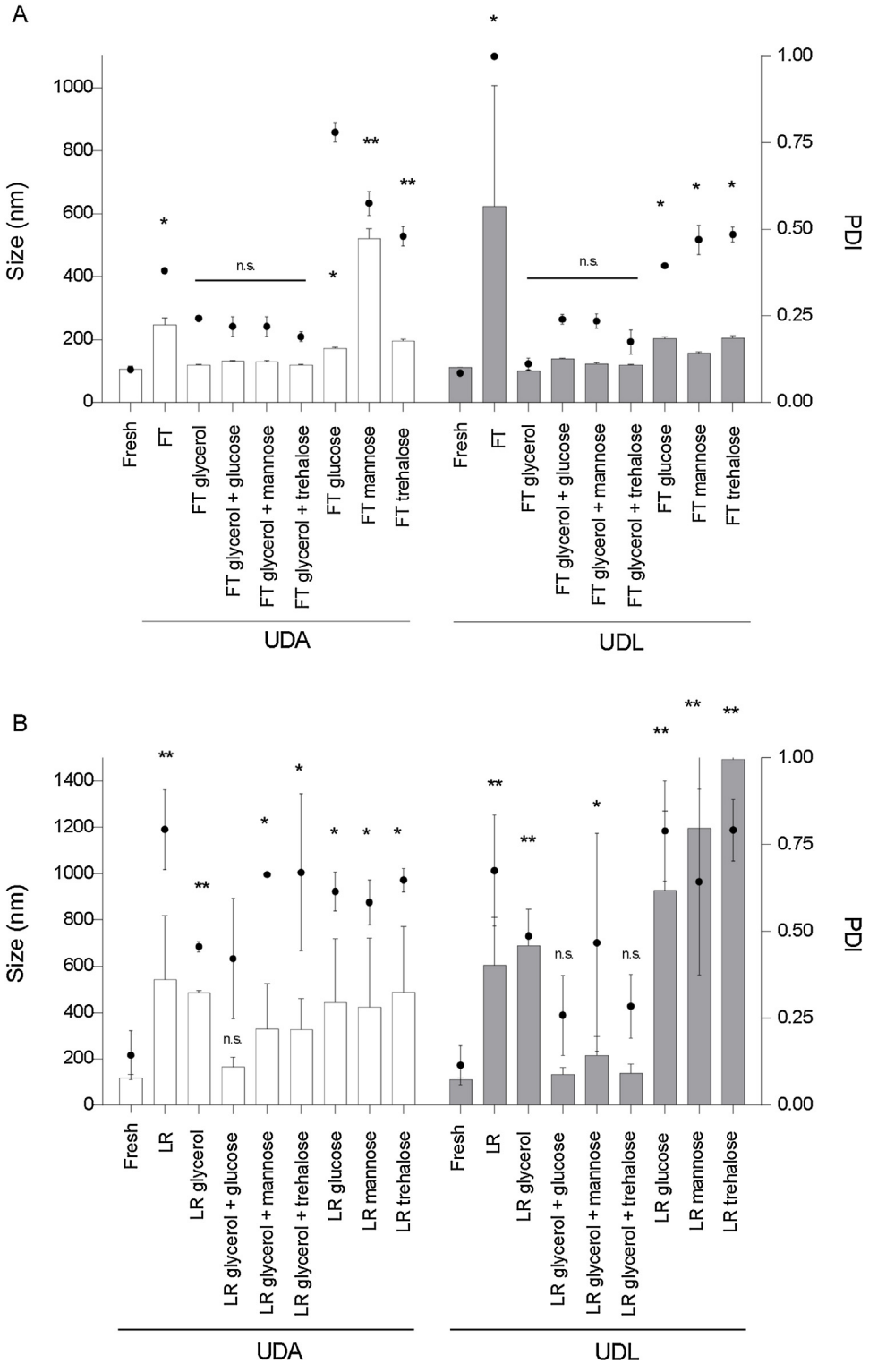

Fig. 1. Effect of cryoprotectants on particle size and polydispersity index of UDA and UDL before and after (A) freeze-thawing (FT) and (B) lyophilisation and reconstitution (LR). Columns show size and dots show PDI. Values are expressed as mean ± S.D (n = 5). Independent two-sample Student t-test against freshly prepared nanovesicles.

its Tm up to −11.5 °C, decreased its ΔH to 0.80 KJ/mol, and upon rehydration, again, the phase transition disappeared.

Unprotected UDL were more sensitive to lyophilization than unprotected UDA. The Tm and ΔH of the gel to liquid crystalline phase transition of lipid bilayers are very sensitive to the lipid packing. Lyophilization caused irreversible reorganization of SPC and NaChol packing in UDL, since Tm and ΔH did not revert to the values of fresh UDL upon rehydration. In contrast, the more packed UDA bilayer suffered less to lyophilization and Tm and ΔH reverted to the values of fresh UDA upon rehydration. Lyophilization of protected nanovesicles, above all, impaired organization changes in the two types of bilayers, but UDL suffered irreversible changes in higher extent compared to UDA.

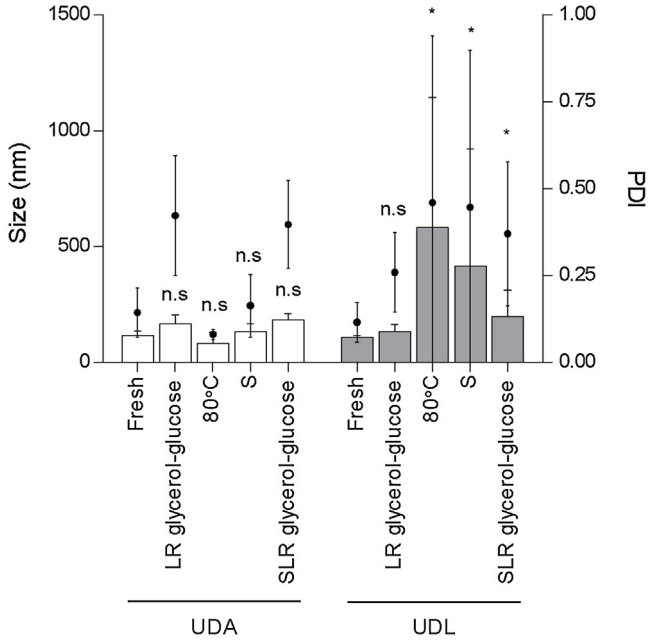

Fig. 2. Effect of incubation at 80 °C, sterilization by autoclaving (S) and sterilization, lyophilization and rehydration (SLR) on particle size and polydispersity index of UDA and UDL. Columns show size and dots show PDI. Values are expressed as mean ± S.D. Independent two-sample Student t-test against freshly prepared nanovesicles.

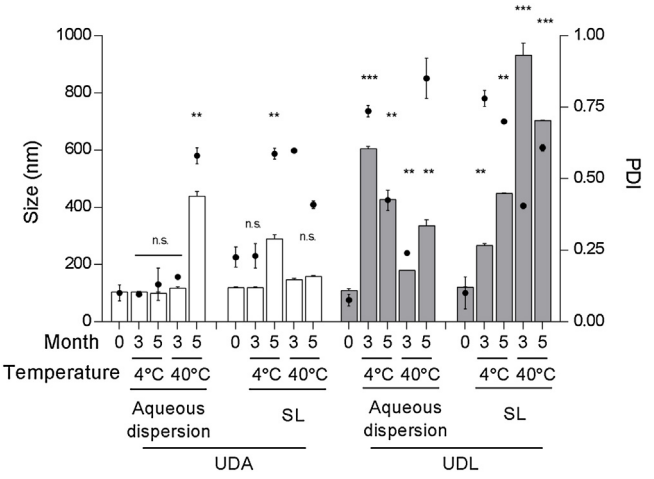

Fig. 3. Colloidal stability of aqueous dispersion or solid sterilized and lyophilized (SL) UDA and UDL upon storageat 4 °C and 40 °C. Columns show size and dots show PDI. Values are expressed as mean ± S.D. Independent two-sample Student t-test against freshly prepared nanovesicles.

Morphology of fresh and lyophilized with glycerol-glucose (protected) and rehydrated UDA and UDL were analyzed by cryo-TEM and TEM. Cryo-TEM micrographs of fresh UDA (Fig. 1S A) and UDL (Fig. 1S C) showed unilamellar nanovesicles of nearly 100 nm diameter which is consistent with the diameter detected by DLS. Cryo-TEM images also revealed some vesicles of sizes between 460 and 40 nm. Besides, UDA and UDL presented not only monolayer morphology but also elongated vesicles, which could be the consequence of the deformable bilayers. Besides, in both samples there were several nanovesicles apparently trapped inside bigger vesicles. LR protected UDA (Fig. 1S B) and UDL (Fig. 1S D) displayed an increase in mean diameter to nearly 300–400 nm without any changes observed in the morphology. TEM images of LR protected UDA (Fig. 1S E) and LR protectedUDL (Fig. 1S F) showed similar trend. Size of LR samples obtained by cryo-TEM and TEM were larger than that obtained by DLS. Due to the different principle of size measurement, results of both techniques cannot be compared directly, but one method assists the other. However, if well we did not found significant increments of the size of LR samples by DLS, we observed an increase of PDI. A constant average size at increasing PDI as measured by DLS can be explained by a wide size distribution as seen in cryo-TEM images.

3.2. Heated or sterilised (autoclaved) nanovesicles

Nanovesicles may lose their colloidal stability after heated during autoclaving [37]. We observed that after 6 h at 80 °C or after sterilized (S) by autoclaving, UDA conserved size and PDI, but size and PDI of UDL were 5 fold increased (Fig. 2). No significant changes in Z potential were detected, but both types of nanovesicles completely lost their HPTS content upon sterilization.

3.3. Sterilised, lyophilized and reconstituted (SLR) nanovesicles

To extend their shelf life, minimize microbial growth and physical chemical degradation, fresh suspension of nanovesicles have to be sterilized and lyophilized. Here nanovesicles were submitted to sterilization by autoclaving (S), added with glycerol and glucose, and then lyophilized (L). When rehydrated (R), size and PDI of $_{SLR}$UDA remained unchanged, while the size of $_{SLR}$UDL was duplicated (Fig. 2).

3.4. Deformability of SLR nanovesicles

The deformability (*D*) of $_{SLR}$ nanovesicles was determined, since topical immunization requires of highly elastic nanovesicles to penetrate the *stratum corneum* of the outer skin. It was found that *D* of $_{SLR}$nanovesicles was similar to that of fresh nanovesicles (4000 and 4600 for UDA and $_{SLR}$UDA respectively, and 4300 and 3800 for UDL and $_{SLR}$UDL, respectively) (Fig. 2S). No significant modification in *D* was detected for nanovesicles mixed with OVA (5300 and 3000 for $_{SRL}$UDA + OVA and $_{SRL}$UDL + OVA, respectively). In all cases, *D*of $_{SLR}$ nanovesicles was significantly higher than that of ordinary non-deformable liposomes (L), characterized by a very low flux of phospholipids [38].

3.5. Stability of nanovesicles on storage

The colloidal stability of aqueous dispersion or solid sterilized and lyophilized (SL) nanovesicles, stored for 5 months at 4 °C or 40 °C, was assessed in terms of size, PDI and Z potential. The colloidal stability of aqueous dispersion UDA remained unchanged up to 5 months at 4 °C and up to 3 months at 40 °C (Fig. 3). Similar results were achieved with solid $_{SL}$UDA, excepting the size was retained up to 5 months at 40 °C. The colloidal stability of aqueous dispersion UDL however, was lost more rapidly. Size at 4 °C and 40 °C increased after 3 months. The size of solid $_{SL}$UDL was 2-fold increased after 3 months at 4 °C and the PDI raised above 0.5; after 3 months at 40 °C its size was 8-fold increased and the PDI raised above 0.5. These results suggest that UDA are more stable to storage at high temperature than UDL; in contrast to $_{SL}$UDL, $_{SL}$UDA could be stored at room temperature with no need of cold chain.

3.6. Immunization

Elastic nanovesicles having antigens partitioned in the membrane or dissolved in the aqueous phase are ordinarily used for topical immunization [14–17]. The inclusion steps of antigens add complexity to the manufacture process, leading to a more challenging and expensive industrial production. For the sake of

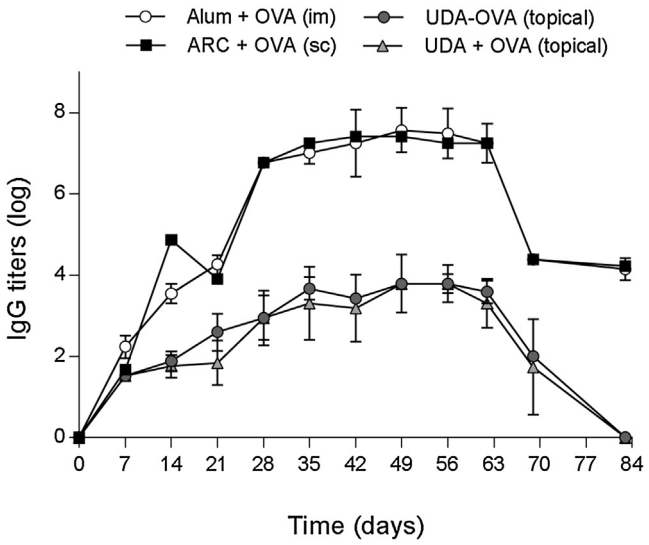

Fig. 4. Serum IgG titers after topical application of OVA included in UDA or mixed with UDA compared to subcutaneous application of OVA mixed with ARC and intramuscular administration of OVA mixed with alum.

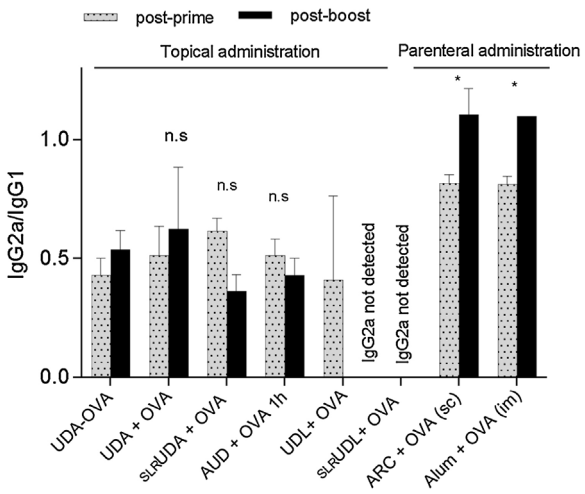

Fig. 6. IgG2a/IgG1 isotype ratio. Dunnett's multiple comparisons test against UDA-OVA.

simplicity, in this work we tested the systemic immune response to nanovesicles mixed with the model antigen OVA. We compared the response upon topical application of OVA mixed with nanovesicles (UDA + OVA) with that of OVA included in nanovesicles (UDA-OVA). We also tested the effect of sequentially topical administration of nanovesicles first and OVA 1 h later. As controls, intramuscular OVA mixed with alum (Alum + OVA) and subcutaneous OVA mixed with archaeosomes (ARC + OVA) were administered. Structural features of nanovesicles used for immunization are shown in Table 1S.

Surprisingly, we did not find significant differences in magnitude and duration of the response of anti-OVA systemic antibodies titers between topical UDA-OVA and UDA + OVA (Fig. 4). The titers after sequential administration of UDA first OVA later, were similar to UDA-OVA in the priming period (day 28), and decreased post-boost (Fig. 5). In agreement with previous results, UDA-OVA and UDA + OVA induced lower titers than intramuscular alum + OVA and subcutaneous ARC + OVA. As expected –because of the presence of TPA in UDA-, the response to UDA-OVA was also 2 log higher than the induced by UDL-OVA.

Then we examined the response to topical administration of $_{SLR}$nanovesicles mixed with OVA ($_{SLR}$UDA + OVA, $_{SLR}$UDL + OVA). We did not find significant differences between titers induced by $_{SLR}$UDA and fresh UDA (Fig. 5), neither between the lower responses to $_{SLR}$UDL and fresh UDL.

No significant differences were found in the IgG isotype balance induced by any formulation of topical UDA (Fig. 6). We observed however that the IgG2a component to topical UDA was lower than the parenteral formulations. Remarkably, $_{SLR}$UDL + OVA did not induce the IgG2a isotype.

Finally, the effect of $_{SLR}$UDA + OVA on cellular immunity was screened by measuring the IFN- γ production in OVA restimulated splenocytes. No differences in INF-γ titers were detected in splenocytes incubated with OVA or culture media, for mice immunized with $_{SLR}$UDA + OVA (Fig. 7). However, these INF-γ titers and those induced by concanavalin A were significantly higher than the equivalent in mice immunized with $_{SLR}$UDL + OVA. Such differences became no longer significant in the post-boost, at expenses of a reduced response to $_{SRL}$UDA + OVA. We also observed that the num-

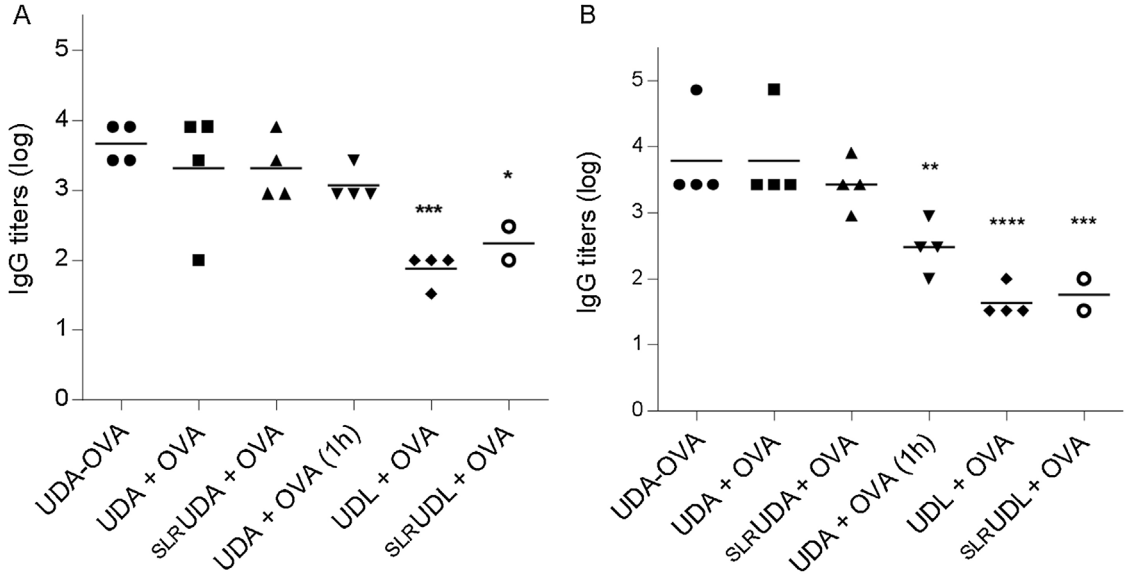

Fig. 5. IgG titers post-prime (A) and post-boost (B) elicited upon topical administration of nanovesicles. Dunnett's multiple comparisons test against UDA-OVA.

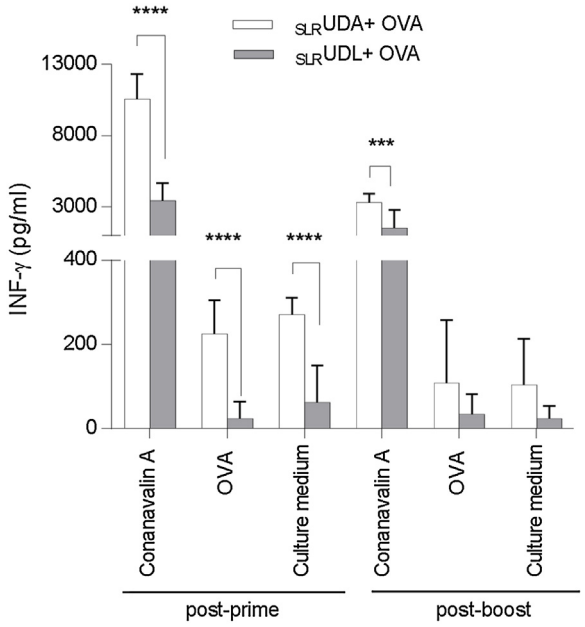

Fig. 7. IFN-γ production by splenocytes after re-stimulation. Values represent mean production ± SD (n = 5).Sidak's multiple comparisons test.

ber of splenocytes from animals immunized with $_{SLR}$UDA + OVA was significantly higher than in mice immunized with $_{SLR}$UDL+ OVA (data not shown). Overall, these results may suggest the induction of a nonspecific cell response to $_{SLR}$UDA + OVA, involving a pro-mitotic activity, together with low titers of pro-inflammatory cytokine, limited to the pre-boost stage.

4. Discussion

Two main factors drive the penetration depth of topical nanovesicles across the intact *stratum corneum*: bilayer elasticity or ultradeformability and size. The ultradeformability results from the reduced Young modulus of the bilayers, that is nearly one order of magnitude lower than that of ordinary non-deformable phospholipid bilayers [19]. The ultradeformability is gained by including a high proportion of edge activators in phospholipid bilayer [39]. Ultradeformable nanovesicles can cross pores of radii smaller than its size without disruption [40]. Experimental evidence supports the existence of an inverse relationship between the size of nanovesicles and their capacity to penetrate the intact skin. For instance, vesicles with size ≥ 600 nm are not able to deliver their content into deeper layers of the skin; those of size ≤ 300 nm are able to deliver their content to some extent into the deeper layers of the skin, while those of size ≤ 120 nm have shown delivery to viable epidermis, and dermis [41]. On the other hand, there is an empiric size pore below which crossing nanovesicles may be disrupted. Intact ultradeformable nanovesicles have been described to penetrate pores of a diameter three fold smaller than their size [42]. Indeed, pores diameter in the *stratum corneum* lipid matrix can be opened without major skin damage merely to 20–40 nm at most [39,43]. Therefore, nanovesicles less than 120 nm – and not higher- have chances to penetrate the skin, it is essential that the size of nanovesicles is maintained around 100 nm along manufacture and storage.

Having this in mind, we recorded the colloidal stability of UDA when submitted to physical stresses suffered in the processes of sterilization, lyophilization and storage. First we determined the colloidal stability of UDA against autoclaving. The most common methods to sterilise materials are the sterile filtration across a 0.2 μm membrane, gamma- irradiation, heat sterilization by autoclaving at 121 °C for 15 min or steam sterilization. While filtration fails to remove virus particles, is time consuming for large sample quantities, and leads to sample loss to the filter, autoclaving is one of the most effective methods to decontaminate harsh material. Liposomes however, suffer structural changes when heated: ordinary liposomes made of diester lipids such as SPC, and cholesterol or pegylated lipids, cannot withhold vesicle size and size distribution when autoclaved [44]. We found here that an aqueous dispersion of UDA could be heated without losing colloidal stability. After autoclaved or incubated 6 h at 80 °C, UDA retained size and PDI. UDL in contrast, suffered aggregation. In our case, UDA maintained size, but the highly water-soluble membrane-impermeant fluorescent dye HPTS was completely lost.

Secondly, we determined the colloidal stability of UDA to lyophilization. Lyophilization is a standard method to remove the water in order to prolong the shelf life of liposomal formulations during storage [45,46]. To prevent vesicle fusion and leakage due to mechanical stress owed to ice crystal formation during freeze, cryoprotectants such as dimethylsulfoxide, glycerol, quaternary amines, or sugars are added [47]. Cryoprotectants may form a protective glassy matrix in which nanovesicles are immobilized, avoiding aggregation, and protecting bilayers from ice crystals. The requirements to protect nanovesicles against drying however, are much more stringent. In this case, lyoprotectants are used to avoid the drying stress suffered during ice formation and unfrozen water removal from nanovesicles. The mechanism of stabilization by lyoprotectants is explained by the water replacement hypothesis [45,48]. Lyoprotectants replace the original water molecules, increase the distance between membranes due to osmotic and volumetric effects, and the inter- and intra- bilayer stress decrease [49]. Most of the molecules used as cryoprotectants are also lyoprotectants. Between 5 and 20% w/v, trehalose, glucose, sucrose or mannitol solutions are the most common cryo- and also lyoprotectants used to protect liposomes. We have previously reported, however that because of its high NaChol content, UDL cannot be lyophilized, not even in high (10 and 20% w/v) sucrose concentration [24]. Here, we speculated that the 0.072% w/v amount of the disaccharide mannose-glucose (provided by the 8.2% w/w of SDGD-5 in TPA), combined with the highly negative charge (provided by the 55% w/w of PGP-Me in TPA), could protect UDA from lyophilization. This assumption resulted partly correct: UDA were more stable than UDL to freeze, but not to dehydration during lyophilization. The results suggest that TPA are partly cryoprotectant, but not lyoprotectant. The full cryoprotection was achieved by adding glycerol. Glycerol is a very well-known cryoprotectant for mammalian cells. Its competitive advantage over sugars is due to its ability to permeate plasma membrane. The osmotic stress in a hypertonic glycerol solution is therefore much smaller than that imposed by a hypertonic sugar solution. Part of the extra-vesicular and intra-cellular water is replaced by glycerol. Hence, the amount of ice formed is lower, the unfrozen fraction remains larger and the degree of shrinkage is limited. Additionally, opposite to sugars that have to be dissolved in the dispersion media of nanovesicles before the bilayers are closed (affecting further manufacturing process such as filter clogging during extrusion), glycerol can be added to already formed nanovesicle suspensions. Additionally, glycerolstably packaged between lipid molecules in the bilayer, establishing hydrogen bonding with phosphate groups in phospholipids, increasing the area occupied per phospholipid molecule [50]. Finally, glycerol is frequently used in topical dermatological preparations because of its moisturizing and smoothing effects, and has been used alone or combined with other agents to lyophilize liposomes [51,52]. To fully protect UDA and UDL from drying stress however, the combination of glycerol with small amount, to keep at minimum the osmotic stress, of glucose was required.

We have hypothesized that because of the TPA content, UDA could display a higher endurance to heat sterilization, lyophilization and storage than UDL. TPA is a natural extract consisting in phosphatidylglycerophosphatemethylester (PGP-Me), sulfated diglycosyldiphytanylglyceroldiether 1-*O*-[α-D-manosa-(2′-*SO*3H)-1′→2′)-α-D-glucosa]-2,3-di-*O*-fitanil-sn-glicerol) (SDGD), sulfated diglycosyldiphytanylglyceroldiether phosphatidic acid (SDGD-5PA), phosphatidylglycerol (PG), and bisphosphatidylglicerol (BPG) [18]. Archaeosomes (nanovesicles fully made of TPA), display higher chemical stability than ordinary liposomes (made of phospholipids), because of the ether linkages, resistant to hydrolysis, the isoprenoid chains without double bonds resistant to oxidation and the *sn*2,3 stereoisomery resistant to stereospecific phopholipases [26]. However, we found that while UDA was more resistant to heat sterilization than UDL, its archaeolipid content was not sufficient to protect them against freeze and dehydration, since in order to lyophilize them, as for UDL, the addition of glycerol and glucose, was required. The storage stability, however were significantly different: size of UDA remained unchanged upon 5 month of storage at 40 °C, while UDL aggregates.

The presence of TPA was responsible for keeping the reduced size of UDA upon SLR-processing required to increase its shelf life. But, while small size favors the skin penetration, the higher titers induced by UDA compared to UDL were owed to the PGP-Me content, the major component of the TPA. PGP-Me is a ligand for the scavenger receptor class A, and responsible for the extensive uptake of nanovesicles containing TPA by macrophages J774A.1 cells (unpublished results). Besides, sugar content of glycolipids such as SDGD and SDGD-5PA in TPA may be recognized by mannose receptors expressed on APC [54].

Finally, we found that topical ultradeformable nanovesicles mixed with antigen prior to administration, elicited an antigen-specific systemic response, allowing to avoid the inclusion steps. Several years earlier, ultradeformable vesicles having ketotifen outside, were reported to significantly improve permeation and skin deposition of the drug over that of vesicles with ketotifen inside. Hydrophilic drugs, thus, might not need to be entrapped in vesicles to penetrate the skin [53]. Our results suggested the same would apply in topical vaccination with voluminous antigens such as OVA. No differences in Th2 biased OVA-specific response topical was found between $_{SLR}$UDA and fresh UDA. If well no specific cellular response was aroused, a non-specific cell mediated response was elicited only by $_{SLR}$UDA + OVA. The steps needed to include antigens in vesicles bilayers or within aqueous space and further purification may be avoided, since the formulation by simple mixing is enough to induce an immune response. We will further address if UDA could be mixed with other antigens different to OVA to elicit an immune response. This finding becomes significant for the industrial manufacture of nanoparticulate vaccines.

Acknowledgments

Authors would like to thank to Mónica Vermeulen from Instituto de Estudios de la Inmunidad Humoral (IDEHU), CONICET-UBA, for technical support for splenocyte isolation. The authors would also like to thank to LME/LNNano for the use of electron microscopy facility and technical support. This work was supported by PICT 2011-2402 ANPCyT and Secretaria de Investigaciones, Universidad Nacional de Quilmes. ATC has a fellowship from Agencia Nacional de Promoción Científica y Técnica (ANPCYT). FP has a fellowship from National Council for Scientific and Technological Research (CONICET). ELR, MJM, APP are members of the Research Career Program from CONICET.

Appendix A. Supplementary data

Supplementary data associated with this article can be found, in the online version, at http://dx.doi.org/10.1016/j.colsurfb.2016.12.039.

References

[1] J. Nicholas, B. Guy, Expert Rev. Vaccine 7 (2008) 1201.
[2] C. Partidos, A. Beignon, V. Semetey, J. Briand, S. Muller, Vaccine 19 (2001) 2708.
[3] J. Hickling, K. Jones, M. Friede, D. Zehrung, D. Chen, Bull. World Health Org. 89 (2011) 221.
[4] S.M. Bal, Z. Ding, E. van Riet, W. Jiskoot, J.A. Bouwstra, J. Control. Release 148 (2010) 266.
[5] N. Kirschner, J. Brandner, N. Ann, Acad. Sci. 1257 (2012) 158.
[6] M. Carstens, Eur. J. Pharm. Sci. 36 (2009) 605.
[7] B. Combadiere, B. Mahe, Microb. Infect. Dis. 31 (2008) 293.
[8] M.-Y. Lee, M.-C. Shin, V.C. Yang, BMB Rep. 46 (1) (2013) 17.
[9] A. Walter, M. Schäfer, V. Cecconi, C. Matter, M. Urosevic-Maiwald, B. Belloni, N. Schönewolf, R. Dummer, W. Bloch, S. Werner, H.-D. Beer, A. Knuth, M. van den Broek, Nat. Comm. 4 (2013).
[10] D. Riminton, R. Kandasamy, D. Dravec, A. Basten, A. Baxter, J. Inmunol. 1 (2004) 302.
[11] A. Harandi, G. Davies, O. Olesen, Vaccine 8 (2009) 293.
[12] A. Paul, G. Cevc, B. Bachhawat, Eur. J. Immunol. 25 (1995) 3521.
[13] A. Paul, G. Cevc, B. Bachhawat, Vaccine 16 (1998) 188.
[14] J. Wang, J. Hu, F. Li, G. Liu, Q. Zhu, J. Liu, H. Ma, C. Peng, F. Si, Exp. Dermatol. 16 (2007) 724.
[15] P. Gupta, V. Mishra, A. Rawat, P. Dubey, S. Mahor, S. Jain, D. Chatterji, S. Vyas, Int. J. Pharm. 293 (2005) 73.
[16] N. Li, L. Peng, X. Chen, S. Nakagawa, J. Gao, Int. J. Nanomed. 6 (2011) 3241.
[17] A. Chopra, G. Cevc, Eur. J. Pharm. Sci. 56 (2014) 55.
[18] L. Higa, P. Schilrreff, A.P. Perez, M. Iriarte, D. Roncaglia, M.J. Morilla, E. Romero, Nanomedicine 8 (2012) 1319.
[19] L. Higa, L. Arnal, M. Vermeulen, A.P. Perez, P. Schilrreff, C. Mundiña-Weilenmann, O. Yantorno, M.E. Vela, M.J. Morilla, E. Romero, PLoS One 11 (3) (2016) e0150185.
[20] D. Carrer, L. Higa, M.V. DefainTesoriero, M.J. Morilla, D. Roncaglia, E. Romero, Colloids Surf. B: Biointerfaces 121 (2014) 281.
[21] A.P. Perez, A. Casasco, M.V. Defain Tesoriero, J.S. Pappalardo, M.J. Altube, L. Duempelmann, L.H. Higa, M.J. Morilla, P. Petray, E.L. Romero, Int. J. Nanomed. 9 (2014) 3335.
[22] C. Alving, M. Rao, N. Steers, G. Matyas, A. Mayorov, Vaccine 11 (6) (2012) 733.
[23] S. Duangjit, B. Pamornpathomkul, P. Opanasopit, T. Rojanarata, Y. Obata, K. Takayama, T. Ngawhirunpat, Int. J. Nanomed. 9 (2014) 2005.
[24] J. Montanari, D. Roncaglia, L. Lado, M.J. Morilla, E. Romero, Int. J. Pharm. 372 (2009) 184.
[25] R. Mohammed, V. Bramwell, A. Coombes, Y. Perrie, Methods 40 (2006) 30.
[26] A. Corcelli, S. Lobasso, in: A.F. Rainey, A. Oren (Eds.), Characterization of Lipids of Halophilic Archaea, Elsevier Amsterdam, 2006.
[27] M.J. Altube, S. Selzer, M. De Farias, R. Villares Portugal, M.J. Morilla, E. Romero, Nanomedicine (Lond.) 11 (2016) 2103.
[28] M. Kates, S.C. Kushwaha, in: S. Dassarma (Ed.), Isoprenoids and Polar Lipids of Extreme Halophiles, Cold Spring Harbor Laboratory Press, New York, 1995.
[29] C. Bötcher, C. Van Gent, C. Pries, Anal. Chim. Acta 24 (1961) 203.
[30] D. Fry, J. White, I. Goldman, Anal. Biochem. 90 (2) (1978) 809.
[31] D. Sprott, S. Sad, L. Fleming, C. Dicaire, G. Patel, L. Krishnan, Archaea 1 (2003) 151.
[32] D. Wessel, U. Flügge, Anal. Biochem. 138 (1) (1984) 141.
[33] B. Van den Bergh, P. Wertz, H. Junginger, J. Bouwstra, Int. J. Pharm. 217 (2001) 13.
[34] A. Boyurn, J. Stand, Clin. Lab. Invest. 21 (1968) 77.
[35] C. Chen, D. Han, C. Cai, X. Tang, J. Control. Release 142 (2010) 299.
[36] W. Shinoda, M. Mikami, T. Baba, M. Hato, J. Phys. Chem. 107 (2003) 14030.
[37] H. Kikuchi, A. Carlsson, K. Yachi, S. Hirota, Chem. Pharm. 39 (1991) 1018.
[38] A.P. Perez, M.J. Altube, P. Schilrreff, G. Apezteguia, F. Santana Celes, S. Zacchino, C. Indiani de Oliveira, E.L. Romero, M.J. Morilla, Colloids Surf. B: Biointerfaces 139 (2016) 190.
[39] G. Cevc, G. Blume, Biochim. Biophys. Acta 1104 (1992) 226.
[40] G. Cevc, D. Gebauer, J. Stieber, A. Schätzlein, G. Blume, Biochim. Biophys. Acta 1368 (1998) 201.
[41] D.D. Verma, S. Verma, G. Blume, A. Fahr, Int. J. Pharm. 258 (2003) 141.
[42] M. Trotta, E. Peira, F. Debernardi, M. Gallarate, Int. J. Pharm. 241 (2) (2002) 319.
[43] A. Oluwatosin, E. Margaret, Z. Sheng, D.J. Pochan, R.L. Bronaugh, S.R. Raghavan, Soft Matter 8 (2012) 10226.
[44] D. Brown, B. Venegas, P. Cooke, V. English, P. Lee-Gau Chong, Chem. Phys. Lipids 159 (2009) 95.
[45] J. Crowe, L. Crowe, in: G. Gregoriadis (Ed.), Liposome Technology, CRC Press, 1993.
[46] J. Crowe, S. Leslie, L. Crowe, Cryobiology 31 (4) (1994) 355.
[47] J. Crowe, J. Carpenter, L. Crowe, T. Anchordoguy, Cryobiol. 27 (1990) 219.
[48] S. Allison, A. Dong, J. Carpenter, J. Biophys. 71 (1996) 2022.

[49] K. Koster, Y. Lei, M. Anderson, S. Martin, G. Bryant, J. Biophys. 78 (4) (2000) 1932.
[50] S. Nakata, A. Deguchi, Y. Seki, M. Furuta, K. Fukuhara, S. Nishihara, K. Inoue, N. Kumazawa, S. Mashiko, S. Fujihira, M. Goto, M. Dend, Colloids Surf. B: Biointerfaces 136 (2015) 594.
[51] A. Rudolph, J. Crowe, Cryobiology 22 (1985) 367.
[52] B. Stark, G. Pabst, R. Prassl, Eur. J. Pharm. Sci. 41 (3–4) (2010) 546.
[53] M. Elsayed, O. Abdallah, V. Naggar, N. Khalafallah, Int. J. Pharm. 322 (1-2) (2006) 60.
[54] L. He, A. Crocker, J. Lee, J. Mendoza-Ramirez, X.-T. Wang, L.A. Vitale, T. O'Neill, C. Petromilli, H.-F. Zhang, J. Lopez, D. Rohrer, T. Keler, R. Clynes, J., Immunol. 178 (10) (2007) 6259.